



LJMU Research Online

Kolivand, H, Al-Rousan, R and Shahrizal Sunar, M

Geometry-based shading for shape depiction Enhancement,

<http://researchonline.ljmu.ac.uk/id/eprint/8076/>

Article

Citation (please note it is advisable to refer to the publisher's version if you intend to cite from this work)

Kolivand, H, Al-Rousan, R and Shahrizal Sunar, M (2017) Geometry-based shading for shape depiction Enhancement,. Multimedia Tools and Applications. ISSN 1380-7501

LJMU has developed **LJMU Research Online** for users to access the research output of the University more effectively. Copyright © and Moral Rights for the papers on this site are retained by the individual authors and/or other copyright owners. Users may download and/or print one copy of any article(s) in LJMU Research Online to facilitate their private study or for non-commercial research. You may not engage in further distribution of the material or use it for any profit-making activities or any commercial gain.

The version presented here may differ from the published version or from the version of the record. Please see the repository URL above for details on accessing the published version and note that access may require a subscription.

For more information please contact researchonline@ljmu.ac.uk

<http://researchonline.ljmu.ac.uk/>

Geometry-based Shading for Shape Depiction Enhancement

Riyad Al-Rousan · Mohd Shahrizal Sunar ·
Hoshang Kolivand.

Received: date / Accepted: date

Abstract Recent works on Non-Photorealistic Rendering (NPR) show that object shape enhancement requires sophisticated effects such as: surface details detection and stylized shading. To date, some rendering techniques have been proposed to overcome this issue, but most of which are limited to correlate shape enhancement functionalities to surface feature variations. Therefore, this problem still persists especially in NPR. This paper is an attempt to address this problem by presenting a new approach for enhancing shape depiction of 3D objects in NPR. We first introduce a tweakable shape descriptor that offers versatile functionalities for describing the salient features of 3D objects. Then to enhance the classical shading models, we propose a new technique called Geometry-based Shading. This technique controls reflected lighting intensities based on local geometry. Our approach works without any constraint on the choice of material or illumination. We demonstrate results obtained with Blinn-Phong shading, Gooch shading, and cartoon shading. These results prove that our approach produces more satisfying results compared with the results of previous shape depiction techniques. Finally, our approach runs on modern graphics hardware in real time, which works efficiently with interactive 3D visualization.

Keywords Non-Photorealistic Rendering · Shape Depiction · Stylized Shading · Curvature

Riyad Al-Rousan

UTM-IRDA Digital Media Centre Media and Game Innovation Centre of Excellence Institute of Human Centred Engineering Universiti Teknologi Malaysia, 81310 Skudai Johor Malaysia.

Department of Software Engineering, Faculty of Computing, Universiti Teknologi Malaysia, 81310 Skudai Johor Malaysia.

E-mail: riyad@magicx.my

Mohd Shahrizal Sunar

E-mail: shahrizal@utm.my

Hoshang Kolivand

E-mail: kolivand@magicx.my

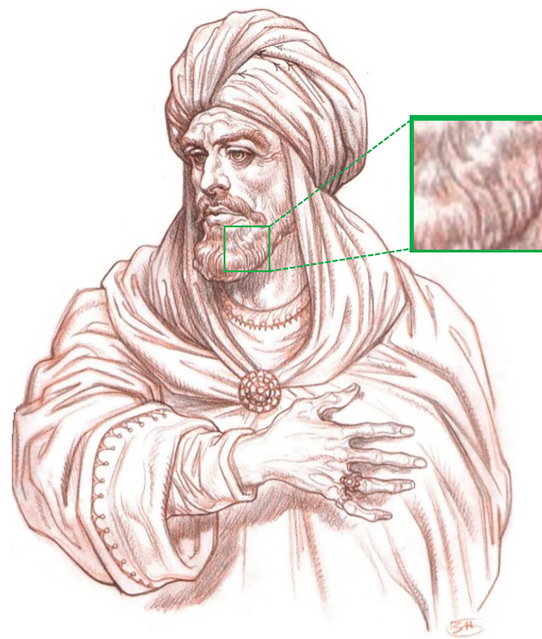
1 Introduction

The advent of computer graphic technologies has not replaced artists. Almost all archaeological, technical and medical books that involve 3D objects have hand-drawn illustrations rather than photographs or computer generated imagery. This lack is evidently highlighted in applications where communication of geometry is primary issue and the aesthetics are the key. Many non-photorealistic rendering techniques have focused on depicting shape through shading to mimic hand-drawn illustration [4, 14, 38]. Compared with hand-drawn illustrations, NPR images still lack the expressive power of many scientific and artistic illustrations. This is due to the ability of skilled artists in conveying shapes through subtle tweaking of shading behavior [32]. As an example, Fig 1 illustrates the exquisite reproduction of garment folds, while the masses of light and shade are efficiently conveyed. It also convincingly illustrates the mans face. Observe how the fine surface details of the forehead region, eyes downwards to the chin are properly depicted.

Previous NPR techniques are not able to depict shapes in a way that similar to artistic drawings. For this reason, more versatile NPR techniques are required to narrow this gap. The proposed technique should correlate the enhancement functionalities to surface feature variations. Moreover, the ability to enhance a wide range of materials (e.g., diffused and specular materials) with respect to specific control on each material type should be taken into consideration. Here, it is really important to intuitively and efficiently control the depiction of 3D objects shape. Other than these issues, an enhancement technique should be also time-efficient to be usable in interactive applications.

The discussed versatile requirements have been recently tackled by techniques that either perturbing the surface normal as in Normal enhancement [2] or altering reflected radiance based on local surface information as in Radiance scaling[33, 34]. Normal enhancement approach proposed convincing enhanced results. However, their enhancement abilities are severely restricted on specific types of material and illumination. Furthermore, Normal enhancement approach is not able to enhance some important geometry features such as concavities and convexities. In contrary, Radiance scaling has shown convincing enhancement abilities without relying on any specific style, material or illumination constraint. It also correlates the reflected lighting intensities to surface feature variations which lead to enhancing the concavities and convexities. Unfortunately, in context of NPR, it tends to mask subtle shading variations, and hence the effectiveness of this technique is a bit reduced in this case. Moreover, the complexity of Radiance scaling function leads to create several rendering errors such as altering the material appearance with badly chosen enhancement parameters.

This paper investigates the problem of communicating surface geometry to viewers. Particularly, enhancing shape depiction through shading, yet without impairing the non-photorealistic appearance. The existing NPR shading techniques that produce rendering results in line with conventional light-



© Burne Hogart

Fig. 1: An example of a artistic shape enhancement. The shape depiction of the character is enhanced by skillfully sketching the shading behavior. Observe how the mans wrinkles are exaggerated and the cloth exhibits multiple folds.

ing models are insufficient to provide geometric features of the same worthy as a hand-drawn illustration [7]. Our goal is to reformulate NPR shading models with respect to geometry surface features. The key idea is to combine the advantages of Normal enhancement and Radiance scaling to relax these constraints. Indeed, previous works in art and visual perception have discussed that (1) Artistic drawings is able to convey the surface feature depending on the depth of perception [5, 6] as in Fig 1, (2) Artistic drawings is able to depict the surface details with great accuracy as in the mans face (see Fig 1)., and finally (3) In artistic drawings, the concavities and convexities are explicitly correlated to masses of light and dark [9] as in Fig 1.

Our technique addresses these three considerations about artistic drawings to enhance the shape depiction. More precisely, the key idea of this paper is two-fold. First, a tweakable shape descriptor is introduced which provides versatile ways of identifying and controlling the salient surface features at multiple scales. Second, a new technique is presented which enhances the shading in a way that depends on both surface normal and surface curvature. The enhancement is achieved in two ways. First, by modifying the surface normal using a simple high-frequency enhancement operation. Second,

by correlating reflected lighting intensity to surface curvature using a new scaling function. Thanks to this scaling function, the rendering is achieved in different enhancement extent, allowing users to produce more desirable enhanced results. On the practical side, Geometry-based Shading technique presents several advantages compared to previous work. 1) It enhances the shape depiction without impairing the non-photorealistic appearance; 2) it works without any constraint on the choice of material or illumination, offering a wide spectrum of NPR styles; and 3) it enhances the surface shape in different ways, enabling a much wider range of enhancement abilities compared to previous work. Specifically, we make the following contributions:

- A robust, view-centered and real-time shape descriptor that reduces the noises while identifying the salient shape features of 3D objects at multiple scales.
- A new non-photorealistic shading technique that reformulates the conventional shading models to provide versatile shape depiction functionalities.

2 Related Work

In order to explicitly enhance object shapes, a wide range of techniques have been proposed. In this section, we provide an overview of these techniques and discuss their abilities for improving the shape depiction.

Although the ample publication of shape depiction enhancement, most of work done focused on line-based rendering techniques. The work of the Saito and Takahashi [25] represents the pioneering effort in this field. Inspired by their approach, many rendering techniques have recently concentrated on depicting the object shape through appropriate set of lines including suggestive contour [3], ridge and valleys [20], apparent ridges [10], abstracted shading [17], [35], demarcating curves [13] and Laplacian lines [36]. These techniques aim at depicting the sharp surface characteristics of an object that correspond to discontinuities of shape features. The limitation of such techniques however is their inability to convey material and illumination with remarkable exception of Lee et al. [17].

Another highly popular approach to depict the object shape is shading. Most of these techniques are inspired from the seminal work that used the ambient occlusion [21] to enhance the shape perception. The goal of such techniques is typically to convey some shape cues that correspond to continuous variations of shape features. For instance, Gooch et al. [7] reproduced lighting effects utilized in technical illustrations. To achieve that, they used cool-to-warm shading tones. The study then was used by other researchers to control the shading effect [1, 28, 27]. These studies had limitations in enhancing the geometric features of shapes.

In order to solve the available problem, many techniques that uses the geometric features to improve object shape explicitly have been proposed. For instance, mean-curvature shading technique [12] used surface curvature to

illustrate shape details. In this process a pair of dark and bright colors are assigned to surface concavities and convexities respectively. The problem that arises here is how to convey the high frequency details of the object shape. Some studies then proposed solutions such as multi-scale mean curvature shading [29]. Then, Vergne et al.[31] tried to develop compelling lighting and shading in real-time using curvature. Vanderhaeghe et al. [30] technique was able to modify stylized shading behavior using geometric features such as curvature. Moreover, the geometry dependent lighting [15] deals with the segmentation of complex models by considering surface curvature. It then makes use of locally consistent lights for improving shape perception. Also, Lee et al.[16] proposed an algorithm for mesh segmentation considers curvatures and uses the GPU to improve the rendering time. This algorithm can also be effective in enhancing the stylized depiction. Vergne et al.[32] presented a technique could enhance the main features of surface with a wide variety of material and illumination attributes. Their technique warps incoming light at each surface point. In other studies,[33, 34] used a technique called radiance scaling for enhancing the shape depiction. This technique considers both surface curvature and material characteristics in order to adjust the reected light intensities. These techniques were efficient in enhancing shape depiction with different kinds of materials and illumination. Furthermore, the 3D gradient enhancement[37] exaggerated visual details using image processing approach. Nevertheless they are unable to enhance some shading techniques such as cartoon shading.

Surface normal is an another geometric feature can be used to enhance the shape depiction. Many techniques exploited this feature. For instance, Cignoni et al.[2] perturbed the high-frequency component of surface normal to enhance the shading effect. By this process they could enhance the shading of regular CAD models. Nevertheless, this technique was not very efficient in case of highly detailed complex shapes. In order to enhance the geometric salient features of the underlying model, Miao et al.[18] incorporated visual saliency measure into normal enhancement operator. In a more recent attempt, they proposed a new definition of visual saliency measure based on multi-channel salience measure [19]. It combined local height distribution, normals difference, and mean-curvature variation. This measure then used in an improved shape depiction of 3D model. Exaggerated Shading [24] is another technique that uses normals at multiple scales. This is to define surface relief based on a Half-Lambertian to produce relief at grazing angles.

To enhance 3D rendering, some studies applied 2D image technique such as unsharp masking. Ritschel et al. [22] tried to extend variation from the normal to the lighting. Their unsharp masking technique increased the contrast of reflected radiance in 3D scenes, which enhanced the depiction of various visual cues. Hao et al.[8] proposed a saliency-guided shading scheme for 3D shape depiction. It enhanced the high frequency of vertex luminance locally to illustrate the details and the overall shape of models.

Although the contributions of these techniques are not deniable, the fact that most of them are incapable to correlate reflected lighting variations to

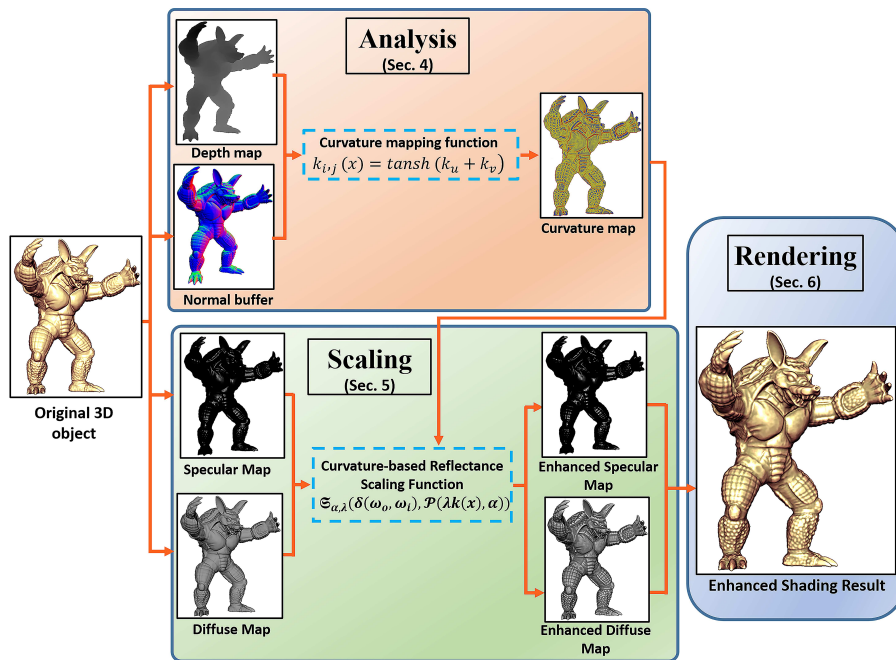


Fig. 2: The rendering pipeline of our approach. It combines estimating the surface curvature, scaling the reflected lighting and rendering the NPR result.

surface feature variations, a remarkable expiation can be observed in [33]. Section 7 discusses the new work in relation to relevant previous techniques.

3 Method

The key to our approach is incorporating surface curvature information into shape depiction enhancement technique. In this paper, we demonstrate the quality of the screen-space curvature under the framework of the normal enhancement scheme [2]. Inspired by image processing, every computation is conducted in image-space; we estimate curvature, scale lighting intensity, and render shapes at each pixel. The process is explained in what follows and illustrated in Fig. 2.

- **3D Shape Description** (Section 4): We first analyze 3D object surface shape via tweakable shape descriptor. The main contribution of this descriptor is extracting salient shape features in a way that exploits the advantages of view-centered curvature tensor of [32] under the framework of the normal enhancement [2]. This provides versatile ways of identifying and controlling the surface salient surface features at multiple scales.

- **Geometry-based Shading** (Section 5): We then introduce a shading technique to enhance the shape depiction. The main contribution of this technique is two-fold: first, we smooth or sharpen the surface normal to attenuate or exaggerate the surface depiction; and then we scale the reflected lighting intensity in a way that depends on surface curvature.
- **Rendering** (Section 6): We finally present various non-photorealistic rendering styles that incorporate the Geometry-based Shading technique. To this end, we reformulate the reflected radiance equation in a way that takes the enhanced shading into account.

4 3D Shape description

Our descriptor is based on the notion of analyzing the surface shape from its enhanced normal field in screen-space. This makes our approach very flexible through computing surface curvature from smoothed normal or exaggerated normal. We developed a new curvature function $k_i(x)$ that allows users to control the curvature around a surface point. As a result, it offers versatile shape depiction functionalities.

4.1 Curvature Analysis

As we wish to enhance the shape depiction through shading, curvature tensor of [32] seemed to be the best choice. This curvature measure is view-centered because it does computations in relation to the direction of view. Hence, it supports some characteristics (e.g., the size of projected features) that are often taken into account by the human visual system. More precisely, it covers the first consideration of artistic drawing considerations. Inspired by their approach, we performed the analysis in 2D. To the end of this paper, we denote by x , y and z the axes of image space. We can define the normal at point x in image space by $n(x) = (n_x, n_y, n_z)$.

To explain the curvature analysis process, it is necessary to explain the definition of normal curvature k_n for smoothing surfaces [23], which is:

$$k_n = (s \ t) \begin{pmatrix} e & f \\ f & g \end{pmatrix} \begin{pmatrix} s \\ t \end{pmatrix} = (s \ t) \mathbf{II} \begin{pmatrix} s \\ t \end{pmatrix} \quad (1)$$

Where $(s \ t)$ corresponds to any vector expressed in terms of a tangent-plane coordinate system and \mathbf{II} is the second fundamental tensor which considers the directional derivatives of normal as can be seen in the following formula:

$$\mathbf{II} \begin{pmatrix} s \ t \end{pmatrix} = (D_u n \ D_v n) = \begin{pmatrix} \frac{\partial n}{\partial u} \cdot u & \frac{\partial n}{\partial v} \cdot u \\ \frac{\partial n}{\partial u} \cdot v & \frac{\partial n}{\partial v} \cdot v \end{pmatrix} \quad (2)$$

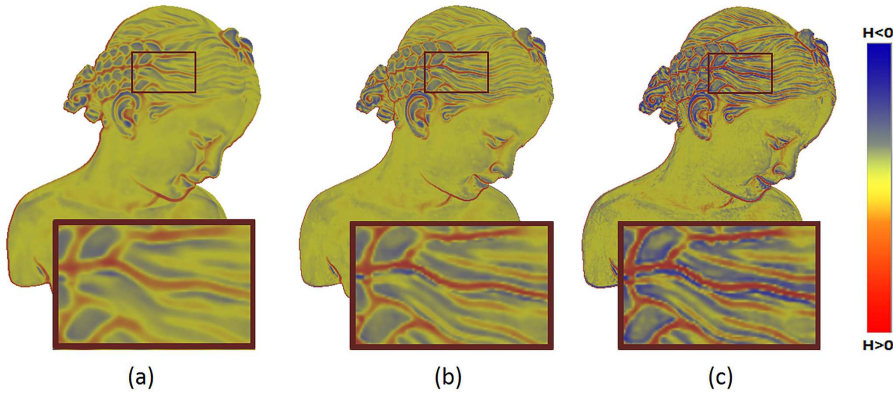


Fig. 3: The process of curvature analysis. (a). The mean curvature obtained from the smoothed normal map. (b) The mean curvature obtained from the original normal map. (c) The mean curvature obtained from the exaggerated normal map. The color scale that was used to visualize the curvature information is illustrated at the rightmost end of image.

In equation 2, $(u v)$ are the axes of an arbitrary coordinate system in the tangent frame. This explains using of image-space filters to the normal map in order to estimate the second fundamental tensors. Accordingly, we compute the Hessian of the depth field by differentiating the gradient with a Sobel filter. The result of this operation is a symmetric 2×2 matrix, in which the eigenvalues corresponds to the maximum and the minimum values of k_n and the eigenvectors corresponds to their directions. We can easily rewrite it as:

$$\mathbf{H} = (u v) \begin{pmatrix} k_u & 0 \\ 0 & k_v \end{pmatrix} \begin{pmatrix} u \\ v \end{pmatrix} \quad (3)$$

where k_u and k_v are the principal curvatures, and $(u v)$ correspond to the principal directions for the curvature tensor \mathbf{H} . Inspired by the way of computing mean curvature measure, a curvature function $m(x)$ is defined as:

$$m(x) = \lfloor (k_u + k_v) \rfloor \quad (4)$$

where $\lfloor \mathbf{x} \rfloor$ is a function that clamps \mathbf{x} to $[-1,1]$. This function describes surface features through remapping mean curvature onto the range value $[-1,1]$, where -1 corresponds to the maximum convexities, 0 to the planar regions, and 1 to the maximum concavities. The result is shown in Fig 3-b. It is clear that concave and convex regions are respectively described in warm and cold hues, while the planer regions in yellow color. The color scale is illustrated at rightmost end of Fig 3.

4.2 Curvature Enhancement

In the process of shape depiction, using normal map contributes to efficient visualization of 3D models. That is why we analyze surface shape from its normal field in screen-space. However, conventional normal map is not appropriate for all illustrative shading styles. On one hand, it cannot visualize the fine details of some coarse 3D models through exaggerated shading style. On the other hand, it may contain extra surface details when used to render cartoon shading style. To tackle this issue, editing a normal-map is an essential step in our approach.

To this end, we enhance the conventional normal map by introducing two normal enhancement operators that provides the user direct enhancement control in real-time. Once the normal is enhanced, the surface shape is analyzed in order to estimate the surface curvature. We conducted two types of normal variations: smoothing and sharpening.

We now show how these variations are used to enhance curvature information. We begin by Normal Smoothing Operator that reduces the high-frequency components of the surface normal (as shown in Fig 4-a.green). To further control of the surface curvature, we utilized the Normal Sharpening Operator that depends on increasing the high-frequency components of the surface normal (as shown in Fig Fig 4-a.red). The two kinds of enhancement operators are addressed in what follows.

4.2.1 Normal Smoothing Operator

The smoothing is performed similarly in 2D over the whole image. Because surface normal is computed for every pixel in image-space, the sharp transitions of surface normal may happen which leads to notable discontinuities in some regions such as between convex and concave regions. We use a smoothing normal operator to avoid such discontinuities, and provide a smooth transition between regions of wide variety of curvature information. For instance, some shading techniques, such as cartoon shading, require to create a saddle at the region between a ridge and a valley. This can be simply achieved by estimating the surface curvature from smoothed normal map. To this end, we apply a Gaussian blur to each pixel in the normal map:

$$n_{sm}(x) = n(x) \otimes g(n(x), \sigma) \quad (5)$$

Where $n_{sm}(x)$ is the smoothed version of surface normal, σ is a scale parameter that controls the amount of blurring, $g(n(x), \sigma)$ is the Gaussian kernel, and \otimes is the convolution operator. We show the original normal map side to side with smoothed version in Fig 5. Note how the details are smoothed in (Fig 6.b) which attenuate the overall appearance of the statues with respect to Fig 5-a.

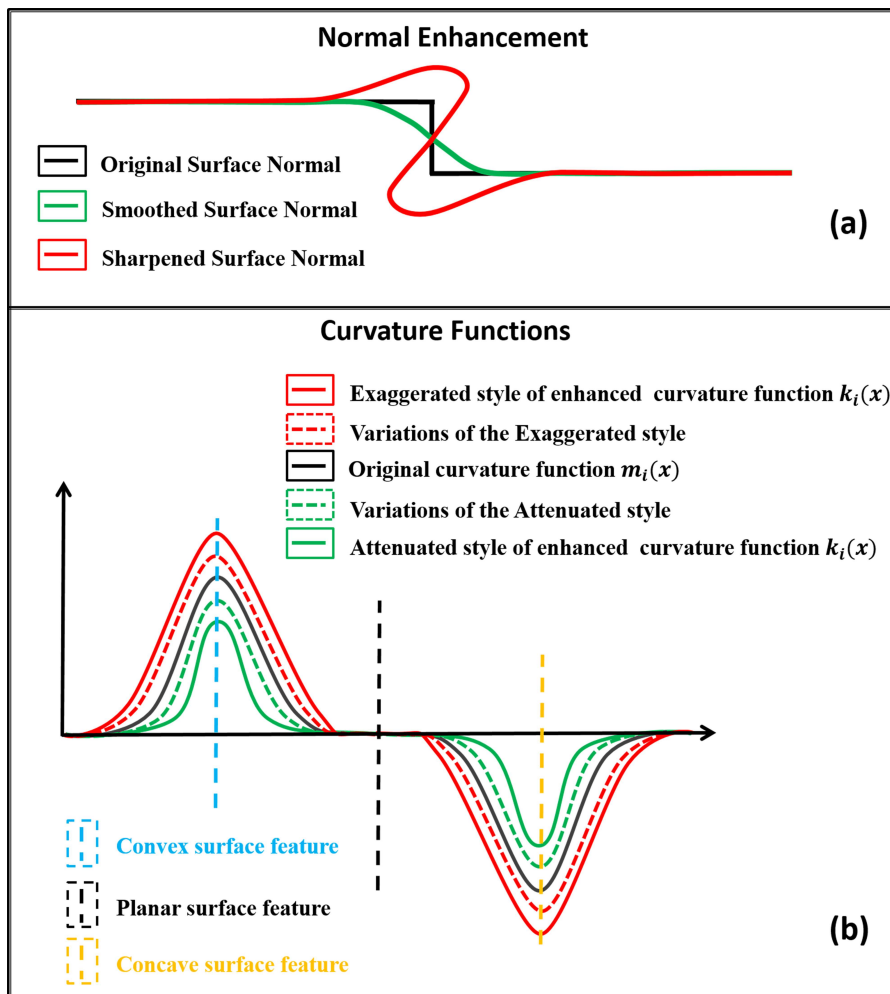


Fig. 4: (a) An enhanced version of surface normal (black line) can be gained through two ways: 1) smoothing the surface normal (green line), or 2) sharpening the surface normal (red line). (b) The dashed vertical lines (in blue, black and orange) represent the surface features (convexities, planar and concavities, respectively). The curvature functions $k_i(x)$ and $k_j(x)$ appear in red and green, respectively. They are created from the enhanced surface normal and they are used instead of $m(x)$ (in black) as they offer better user control. The dashed green lines represent variations of surface normal attenuation, while the dashed red line represents the variations of surface normal exaggeration. In our approach, we use the former method for cartoon shading and the latter for exaggerated shading.

Given a smoothed version of surface normal (Shown in Figure 4-a.green), we then compute a new surface curvature function $k_j(x)$ (Shown in Fig 4-b.green) in the same way as equation 5. The difference here is that the Hessian matrix is computed from the smoothed normal map. Compared to original curvature function $m(x)$ that sometimes convey curvatures more than what the shading techniques are need, the new curvature function $k_j(x)$ allows us to only convey the curvature of nearby features as can be seen in Fig 4-b.green. Such enhancements may also depict some surface details, but they are efficient in improving shape depiction. From a practical perspective, the new curvature function $k_j(x)$ offers some advantages. It avoids discontinuities between surface curvature regions and allows users to control the amount of surface features by tweaking scale parameter σ .

4.2.2 Normal Sharpening Operator

Our goal in this part is to enhance the curvature function $m(x)$ to convey more surface features. To this end, we use the unsharp masking approach. Unsharp masking is a filter that amplifies the high-frequency components of a signal $n(x)$ by adding back the difference between $n(x)$ and a smoothed version $n_s(x)$ of the original signal. It can be achieved through the following equation:

$$n_{sh}(x) = n(x) + \lambda(n(x) - n_s(x)) \quad (6)$$

In our approach, $n(x)$ is the surface normal at point x in image space. The Gaussian filter is used to obtain the smoother version of the normal $n_s(x)$. For simplicity, we denote the difference between the original and smooth normals as the contrast normal $C(S) = n(x) - n_s(x)$. The desired result of a high-frequency enhancement $n_{sh}(x)$ can be obtained if $C(S)$ component is added to the original mesh. The process is depicted in Fig 5. Note how the details are sharpened in (Fig 5-d) to improve the overall appearance of the statues with respect to (Fig 5-a). More precisely, unsharp masking by enhancing high-pass components of normal would exaggerate the surface normal (Fig 4-a (red)). Two efficient parameters can enhance the curvature function. The first parameter is σ in equation 6, which is used to modulate the smoothness of surface normal. The other one is the user-controlled parameter λ , which is used to perturb the original surface normal. Fig (4-b (red)) illustrates the curvature function $k_i(x)$ which is computed similar to equation 5. The main difference is computing the Hessian matrix from the exaggerated normal map. The new curvature function $k_i(x)$ contributes to accurate conveying the curvature of far features and precise user control. It is clear in Fig 5.b that the highest values of $m(x)$ (in black) mostly appear in very near to each feature location.

An important advantage of $k_{i,j}(x)$ over $m(x)$ is the ability to control the sharpness of concave and convex regions. This advantage thus offers versatile shape depiction functionalities.

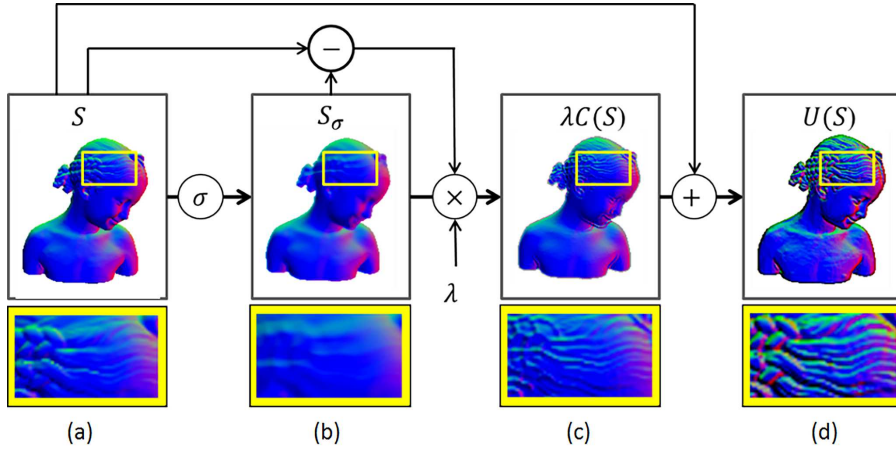


Fig. 5: The process of unsharp masking. (a) The original normal S ; (b) The smoothed version of surface normal S_σ ; (c) The λ -scaled difference between the original and a smoothed version $C(S)$; The final unsharp image $U(S)$.

4.3 Implementation

In practice, our shape analysis is performed per-pixel entirely on the GPU using multiple passes. The normal buffer and depth buffer are used as input, and output our enhanced curvature map in another buffer. It consists of multi-scale normal differentiating (Hessian H_s). In **Algorithm 1**, x denotes the current pixel and N_r its $r \times r$ pixel neighborhood. There are essentially several steps in the algorithm. Normal map (1) is generated using OpenGL Shading Language. We render the normal map into G-buffers on the GPU. As a result of this stage, we obtain texture that contains the normal map. The enhanced normal map S' is produced using special normal operators in step (2). We found that using Gaussian blur gives accurate results for smoothing, as well as unsharp masking for exaggerating. Also in step (2), the relationship between the surface normal $n(x) = (n_x, n_y, n_z)$ and the depth $d(x)$ is defined as follows: $D_s(x) = (-n_x/n_z, -n_y/n_z, n_z, depth)$ as explained in [32]. The ring of neighbors N_r in (3) is computed based on the simple formula $N_r = r \times r$ where $r = 2r + 1, \forall r \in \mathbb{N}^+$. At step (4), The Hessian matrix is computed by differentiating the multi-scale depth gradient normal map with a Sobel filter. Finally, the mean curvature is mapped to the range $[-1, 1]$ via \tanh function.

5 Geometry-based Shading

The goal of the Geometry-based Shading technique is to enhance the shape depiction of 3D objects in real-time. Geometry-based Shading is based on the premise that combines the advantages of Normal enhancement approach and curvature shading approach. This combination would yield better NPR

Algorithm 1 Multi-scale screen-space mean curvature estimation

1. Uploading the 3D mesh model M as input
2. $S \leftarrow$ Generating the surface normal map
3. $S' \leftarrow n_{sm}(S), n_{sh}(S)$
4. $N_r \leftarrow$ Find the neighborhood at scale r
5. $H_s(x) \leftarrow$ Sobel Filter ($S'(N_r)$)
6. $k_{i,j}(x) \leftarrow \tanh(k_u + k_v)$

depiction. Moreover, it can be manipulated easily by users, and applied to a wide spectrum of styles. Geometry-based shading technique covers the second and third artistic principles, which proposed in the introduction. It scales the intensity lighting to concavities and convexities regions and exaggerates or attenuates the surface details, while at the same time conserves the overall object appearance.

5.1 Curvature-based Reflectance Scaling Function

In [11], the reflected radiance L_r at a surface location x in direction w_o is represented by:

$$L_r(x, \omega_o) = \int_{\Omega_n} L_i(x, \omega_i) \rho(x, \omega_o, \omega_i) \langle n(x), \omega_i \rangle^+ d\omega_i \quad (7)$$

Where Ω_n is the upper hemisphere oriented around the surface normal $n(x)$ at x , $\rho(x, \omega_o, \omega_i)$ is bidirectional reflectance function (BRDF), $\langle \cdot \rangle^+$ is a dot product that is clamped to zero, and L_i is the incoming light. Unfortunately, Equation 7 cannot directly be amended to adjust reflected light intensity based on surface curvature. Therefore, reformulating the reflectance radiance equation in terms of correlating the reflected lighting intensity to surface features is mandatory. To this end, we propose a new Curvature-based Reflectance Scaling Function that able to brighten the areas of convex features, while the areas of concave features are darkened.

The presented Curvature-based Reflectance Scaling Function \mathfrak{S} is a short notation for $\mathfrak{S}_{\alpha, \lambda}(\delta(\omega_o, \omega_i), P(\lambda k(x), \alpha))$ that consists entirely of two functions: intensity mapping function and curvature mapping function. The intensity mapping function $(\delta(\omega_o, \omega_i) : \Omega^2 \rightarrow [0, 1])$ computes normalized reflected lighting intensity, where 0 corresponds to minimum reflection and 1 to maximum reflection. The second part $P_{\lambda, \alpha}(k)$ is curvature mapping function. The goal of this function is to boost the weak features or attenuate the strong features by controlling the enhancement location and the curvature magnitude. To this end, we introduce the following non-linear mapping function:

$$P_{\lambda, \alpha}(k) = \text{pow}(\lambda |k|, \alpha) \quad (8)$$

Where $k(x) : \mathbb{R}^3 \rightarrow [-1, 1]$ represents our proposed function to estimate and enhance the surface curvature, where -1 corresponds to maximum convexities, 0 to planar regions, and 1 to maximum concavities. The precise definition of this function is provided in Sec.4. The main interesting property of $P_{\lambda, \alpha}(k)$ is the way of controlling the curvature spreading over surface shape is easily controlled via two parameters. The first parameter is $\lambda \in [0, \infty]$, which is used to control the curvature magnitude. The other one is $\alpha \in (0, \infty)$ that controls the curvatures spread over the surface model. Fig 6-a shows the curve of the power function. Note that the value parameter α gives intuitive variations for exaggeration ($\alpha < 1$) as well as attenuation ($\alpha > 1$).

Once the intensity mapping function ($\delta(\omega_o, \omega_i)$) and curvature mapping function $P_{\lambda, \alpha}(k)$ are defined, we propose a coherent formula for mapping them in the reflectance radiance equation 7. In spirit, this function is similar to the emphasis function of [31], except that instead of altering a user-controlled parameter to tweak the surface curvature, we aim to correlate the reflected lighting intensity to surface curvature. Hence, we rewrite their function as follows:

$$\Theta(\delta, P) = \frac{\delta}{e^P(1 - \delta) + \delta} \quad (9)$$

This function explicitly correlates reflected lighting intensity $\delta(\omega_o, \omega_i)$ to surface curvature $P_{\lambda, \alpha}(k)$. Fig 6-b shows the important advantages of this function. It is important to note that this function is equal to the original

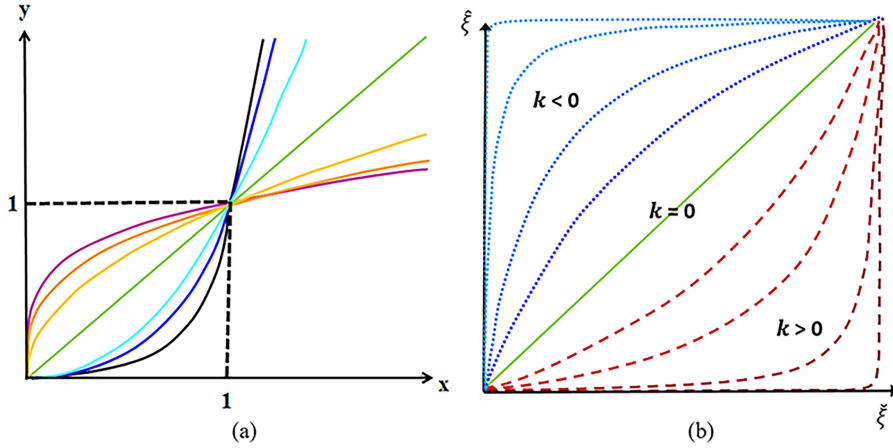


Fig. 6: The analysis of the enhancement function: (a) Power curve, using different values of α (0.25, 0.33, 0.5, 1.0, 2.0, 3.0, 4.0). (b) *Intensity mapping function*, using different values of k . Observe how the variations of curvature values increase or mitigate the value of reflected intensity, while keeping a range between $[0, 1]$. Note that when $k = 0$ (i.e., in planar surface regions), this function does not have any influence on the reflected intensity.

reflected lighting intensity only when $k = 0$ as required. In other words, in the absence of surface feature (i.e. in planar surface regions), the function should not affect the reflected lighting, and therefore $\mathfrak{S}(\delta, P) = \delta$. Moreover, for concave features ($k > 0$), reflected lighting intensities at concave features δ are darkened depending on the value of concave features. For convex features ($k < 0$), the opposite effect is obtained where the reflected lighting intensities at convex features are brightened based on the value of convex features δ . The other remarkable advantage is that only the curvature parameter affects the reflected lighting intensity.

5.2 Normal enhancement guided shading enhancement technique

The key idea of normal enhancement approach is to improve the shading of 3D models by dynamically perturbing the surface normals. This paper makes use of this approach to improve the visual perception of the 3D models. Cignoni et al.[2] have shown that making use of high-frequency enhancement operation of the surface normals would enhance the original shape details without impairing the desired appearance. As a result, we were encouraged to use normal enhancement approach in shape depiction enhancement. To achieve this goal, we have incorporated the enhanced surface normal $n'(x)$ into reflected radiance equation. This modification is given in equation 11. Thanks to the enhancement normal operators as explained in Section 4.1., the new normal map provides different enhancement abilities that would allow users to improve the shape depiction.

To achieve this goal, we have incorporated the enhanced surface normal $n'(x)$ into reflected radiance equation. This modification is given in equation 11.

5.3 Implementation

Geometry-based shading technique is computed per-pixel on the GPU. We take the enhanced curvature buffer as input, and render the final output on screen. It consists of enhancing the surface curvature as mentioned in Section 4. According to the aforementioned enhancement phases, we now summarize the main steps of Geometry-based Shading Technique in **Algorithm 2**.

6 Non-Photorealistic Rendering Styles

The final phase in our approach is to render 3D objects without any constraint on the choice of material or illumination, while taking into consideration the way of Geometry-based Shading technique that enhances the lighting at each surface point. We demonstrate our approach with three different non-photorealistic shading styles: Blinn-Phong Shading, Cartoon shading and Gooch Shading.

Algorithm 2 Geometry-based Shading Technique

-
1. Uploading the 3D mesh model M as input
 2. $S \leftarrow$ Generating the surface normal map
 3. $S' \leftarrow n_{sm}(S), n_{sh}(S)$
 4. $k_{i,j}(x) \leftarrow \text{tansh}(k_u + k_v)$
 5. $\mathfrak{S}_{\alpha,\lambda}(\delta(\omega_o, \omega_i), P(\lambda k(x), \alpha)) \leftarrow$ Scaling the reflected intensity δ based on $k_{i,j}(x)$
 6. $L'_r(x, \omega_o) \leftarrow$ Reformulating $L_r(x, \omega_o)$ with respect to $\mathfrak{S}_{\alpha,\lambda}(\delta(\omega_o, \omega_i), P(\lambda k(x), \alpha))$ and $n'(x)$
 7. $L'_r(x, \omega_o) \leftarrow$ Reformulating the non-photorealist shading models with respect to the choice of $\delta(\omega_o, \omega_i)$
-

The lobes of such shading models are defined in the $[0,1]$ range; hence, mapping the mean curvature into this range should be achieved. To this end, the function of step (6) in algorithm 1 becomes:

$$k_{i,j}(x) = 0.5 + 0.5 \times (\text{tansh}(k_u + k_v)) \quad (10)$$

We then propose a reformulation of equation 7 to take the Geometry-based Shading technique into account:

$$L'_r(x, \omega_o) = \int_{\Omega_n} L_i(x, \omega_i) \rho(\omega_o, \omega_i) \mathfrak{S}(x, \omega_o, \omega_i) \langle n'(x), \omega_i \rangle^+ d\omega_i \quad (11)$$

Where L'_r is the enhanced reflected radiance, $n'(x)$ is the enhanced surface normal, $\mathfrak{S}(x, \omega_o, \omega_i)$ is the proposed Curvature-based Reflectance Scaling Function.

Once the reflected radiance equation is reformulated in order to adjust reflected light intensity in a way that depends on surface normal and surface curvature, we then demonstrate how the Geometry-based Shading technique is adapted to various NPR styles by a proper choice of intensity mapping function δ .

6.1 Blinn-Phong Shading model

In the context of non-photorealistic rendering, it is common to make use of simple shading models such as Blinn-Phong shading model. Geometry-based shading technique can alter surface shading to enhance surface fine-scale geometric details in a non-photorealistic manner. This process is performed by incorporating enhanced surface normal and surface curvature measure into Blinn-Phong shading model.

Before incorporating Curvature-based Reflectance Scaling Function into Blinn-Phong shading model, the choice of reflectance mapping function δ should be explained. The lobes of Blinn-Phong shading model are defined in

the $[0,1]$ range. Subsequently, it is best to utilize them directly as mapping functions: $\delta_j = \rho_j$. Now with single light direction and Blinn-Phong shading model, equation 11 becomes :

$$L'_r(x, \omega_o) = \sum_j \rho_j(\omega_o, \ell) \mathfrak{S}_j(x, \omega_o, \ell) L_j(\ell) \quad (12)$$

where $j \in \{a, d, s\}$ iterates over the components of Blinn-Phongs shading model: ambient, diffuse, and specular and ℓ is the direction of light source at point x . L_j corresponds to light intensity of each component of Blinn-Phongs shading model, with notable exception of L_a (L_a is a constant). $\rho_a = 1$, $\rho_d(\ell) = (n' \cdot \ell)$ and $\rho_s(x, \ell) = (n' \cdot r)^f$, were respectively given to the ambient, diffuse and specular components. Here, $n'(x)$ corresponds to enhanced surface normal. Also, $r = \frac{\ell + v}{\|\ell + v\|}$ corresponds to the reflection direction in which the view direction represents by v and the shininess parameter represents by $f \in [0, \infty]$. $\mathfrak{S}_j(x, \omega_o, \ell)$ corresponds to the Curvature-based Reflectance Scaling Function for each light.

The Curvature-based Reflectance Scaling function is not only correlates reflected lighting intensity to surface feature variations, but also enables users to control each term of Blinn-Phong shading model independently with individual scaling parameters. For instance, observe how the specular material are properly reflects a highlight in both: concavities and convexities. This en-

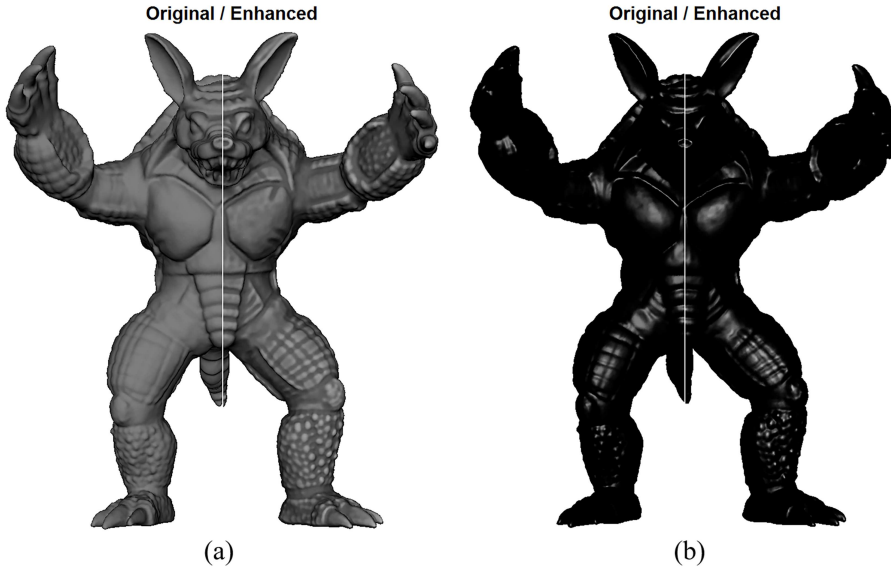


Fig. 7: Geometry-based shading technique enhances each layer of Blinn-Phong shading model independently. (a) Diffuse material is enhanced independently. (b) Specular material is enhanced independently.

hancement is done if the reflected light intensity in convex regions increased and those in concave ones are decreased (see Fig 7-b). Diffuse layer is another type of material can be enhanced. Fig 7-a illustrates the results of enhancing the diffuse layer. It is clear that concave and convex regions are respectively depicted in dark and bright colors. Fig 8 shows some of the results we achieve by using Geometry-based Shading technique with Blinn-Phong Shading Model. It based on combining both enhanced components (diffuse and specular). Observe how the overall appearance of 3D object are properly enhanced based on both surface features and material characteristics.

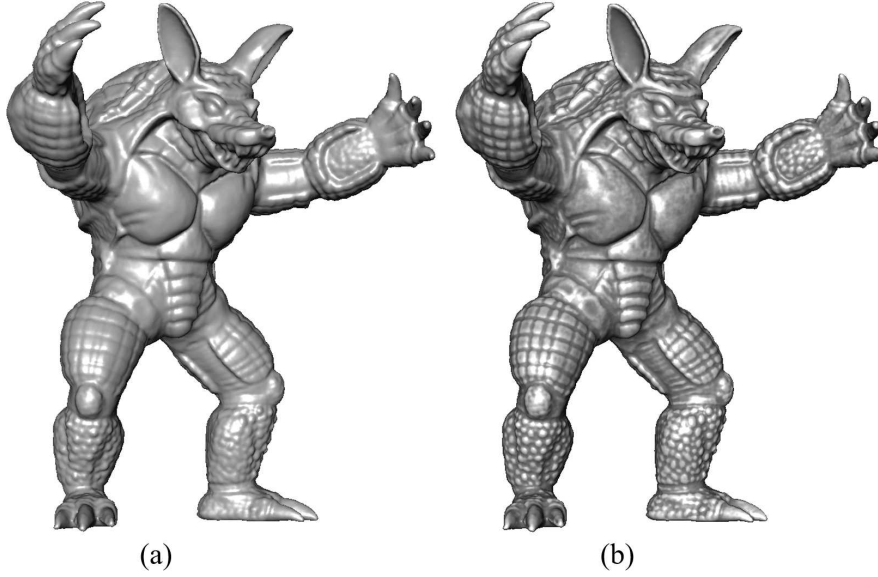


Fig. 8: Geometry-based shading technique enhances Blinn-Phong shading model. (a) Original Blinn-Phong shading models. (b) Enhanced Blinn-Phong shading model. Observe how Surface features and material characteristics are taken into account when enhancing each lobe of Blinn-Phong shading model.

6.2 Cartoon shading

Cartoon shading consists of quantizing the amount of diffuse shading and mapping each discrete value to a different color. Consequently, in order to apply Geometry-based shading technique to cartoon shading style, the choice of reflectance mapping function should be consistent with this finding. To this end, we quantize the reflected diffuse intensity using the following formula:

$$\delta_d = \frac{\lfloor (0.5 + (Q_L \times pow(\rho_d, r))) \rfloor}{Q_L} \quad (13)$$

Where δ_d corresponds to reflected diffuse intensity that we use in cartoon shading style, $r \in [0, 1]$ which is a power level can be used to enhance the intensity of color, Q_L is the quantization level parameter and $\lfloor x \rfloor$ is a function that returns the largest integer less than or equal to x . The choices of δ_d and δ_s are chosen in the same way as Blinn-Phong shading model. The end result is a convincing cartoon style that works with wide range of materials and introduces enhancement abilities for conveying geometric features (see Fig 9). Contrary to radiance scaling [34] and light warping [32], which tends to mask subtle surface features, Geometry-based shading technique enhances the salient surface features while preserving the overall appearance of 3D objects.

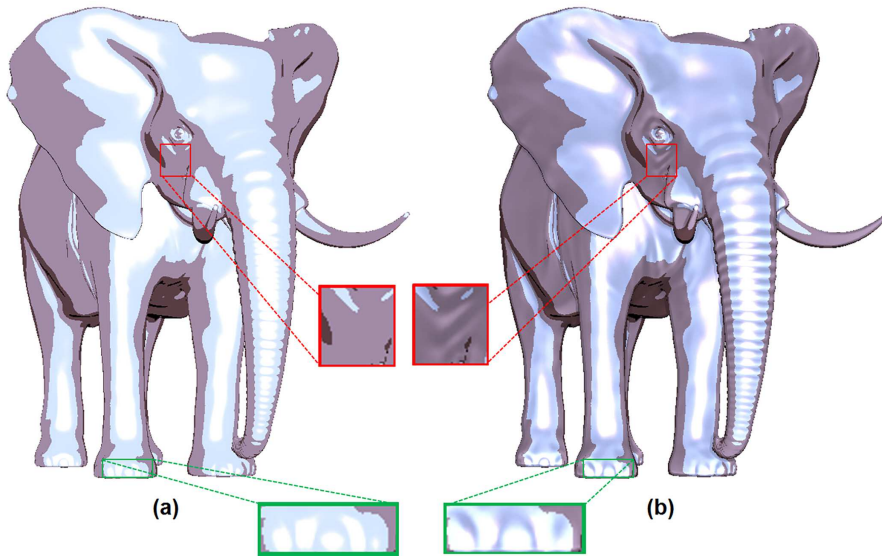


Fig. 9: Geometry-based shading technique enhances cartoon style: (a) Conventional cartoon shading. (b) Enhanced cartoon shading. Observe how the quantized reflected intensity is scaled to reveal shape features such as details in the elephant trunk, leg and around eye of the elephant model.

6.3 Gooch shading

Another place where a Geometry-based Shading technique is needed is when using blending between colors to convey the shape. The main idea in [7] is to create cool-to-warm transition for technical illustration. To properly scale the cool-to-warm shading, we use Geometry-based shading technique with Gooch shading style. Our choice to compute the intensity mapping function is inspired by their approach:

$$\delta_j = \left(\frac{1 + \rho_j}{2} \right) k_{cool} + \left(1 - \frac{1 + \rho_j}{2} \right) k_{warm} \quad (14)$$

Where $j \in \{a, d, s\}$ iterates over the ambient, diffuse, and specular component of Gooch shading model. ρ_j is computed based on Blinn-Phong shading model. k_{cool} and k_{warm} correspond to cold and warm colors of Gooch shading model (see [7]). With Geometry-based Shading technique, we can properly enhance the shape depiction by assigning a pair of warm and cold colors to surface concavities and convexities, respectively, as shown in Fig 10. Observe how the various surface features are properly enhanced in the ear, around the eye and the hair of bimba model.

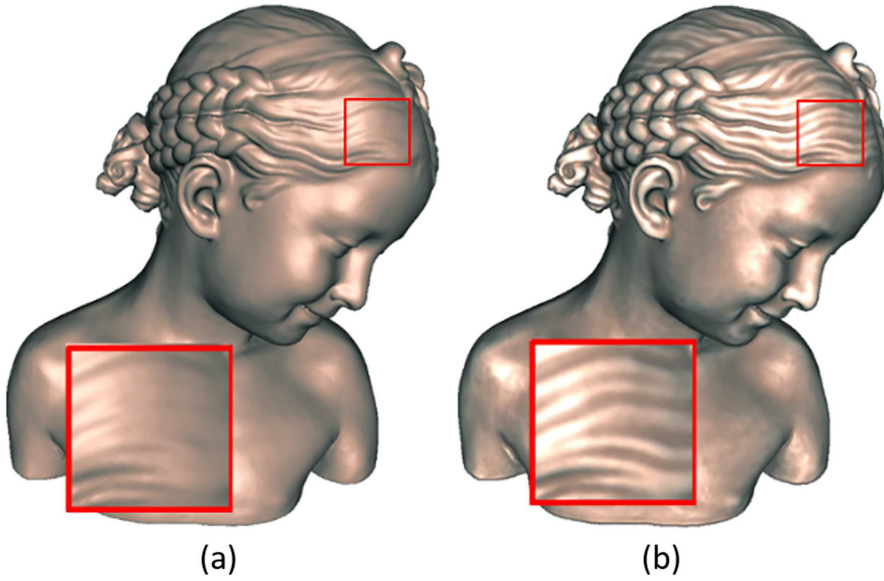


Fig. 10: Geometry-based shading enhances Gooch style: (a) Original Gooch shading model. (b) Enhanced Gooch shading model.

7 Results and analysis

As enhancing the shape depiction in a way that depends on geometry features is the main goal of our technique, it is axiomatic to select 3d models that have mathematical features of particular interest (e.g. concavities, convexities and planer regions). More precisely, it is preferred to select 3D models that have many curved surfaces and fine details. Accordingly, we select 3d models such as Armadillo, Bimba, Elephant and Gargoyle which cover a wide variety of these mathematical features. In a nutshell, we perform experiments using 3D

models with high geometrical features to confirm that the geometry-based shading technique has the potential to enhance the surface details.

Screen-space approach is used to compute our measure of curvature. As a result, natural simplification behaviors are produced, which yields to better results compared with the object-space curvature measures. Specifically, our curvature measure is able to convey the details in the closer objects more than in the farther ones. This advantage is a vital propriety in human visual system and it is illustrated in Fig 11.

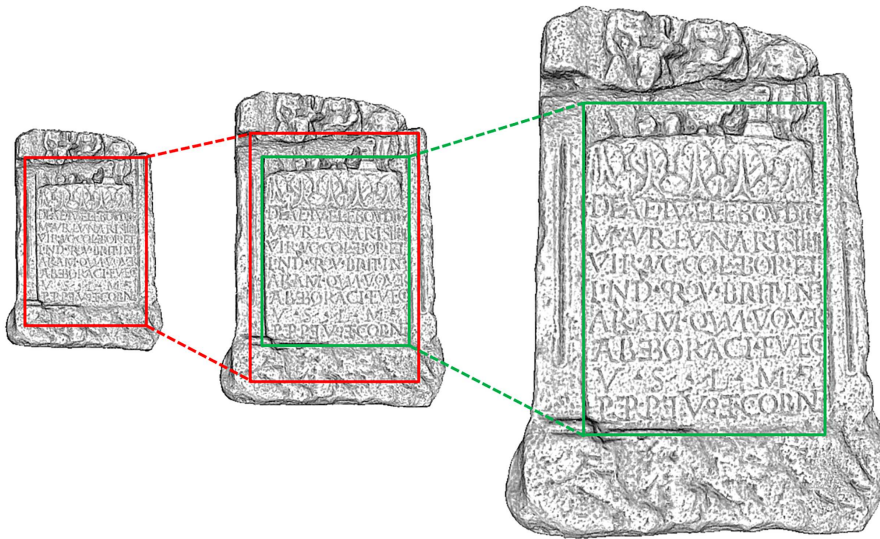


Fig. 11: Geometry-based Shading technique using screen-space descriptor. This is a comparison between the detected features that computed at three different scales. Observe how these features depend on the viewpoint.

An important advantage of our shape descriptor is the robust describing of the surface features, which produces improved results in various rendering settings. As an example, observe the lion model in Fig 12. Conventional curvature Fig 12-a describes the concavities and convexities in precise way and thus allow to improve shape depiction. However, the end result is too noisy (see Fig 12-b). The tweakable shape descriptor avoids such limitation as it smooths the surface normal in prior of estimating the surface curvature. Hence, it exhibits less noise and produces smooth transitions between curved and planar regions (see Fig 12.c). Consequentially, Geometry-based Shading technique produces coherent and clear shading results for any choice of curvature function (see Fig 12.d).

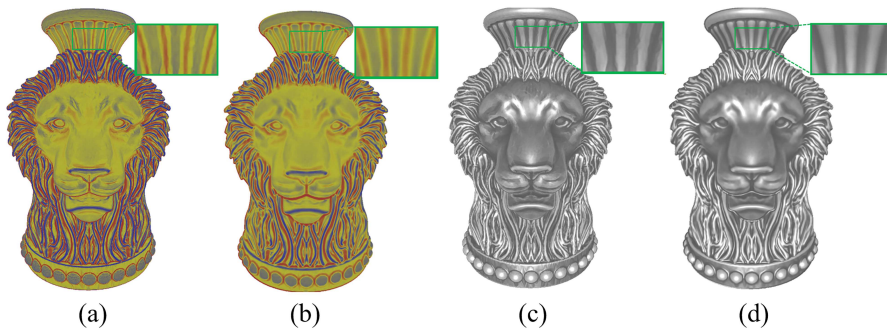


Fig. 12: Robustness to noise. (a) Conventional surface curvature. (b) Enhanced result after conventional curvature guided Blinn-Phong shading model. (c) Smoothed surface curvature. (d) Enhanced result after smoothed curvature guided Blinn-Phong shading model.

Fig 13 shows how Geometry-based Shading technique enhances the surface depiction of an input 3D model in two different illumination settings. Observe how the improvement remains coherent, while the number of light samples is completely different in each case. It is clear that in both settings, the surface features are properly enhanced: the wings, around the eyes and the base of gargoyle. Indeed, the details are enhanced with the notable ability to distinguish convexities from concavities regardless of illumination settings.

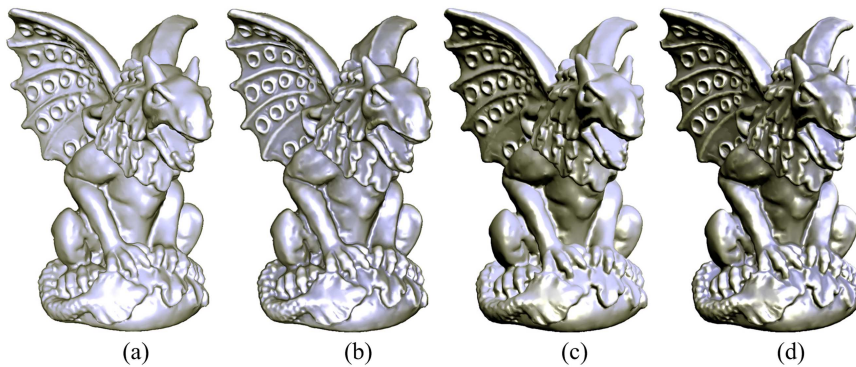


Fig. 13: Geometry-based shading technique enhances shape depiction using different illumination settings. (a) The original rendering without enhancement using single light direction. (b) Our enhanced results using single light direction. (c) The original rendering without enhancement using multiple light directions. (d) Our enhanced results using multiple light direction.

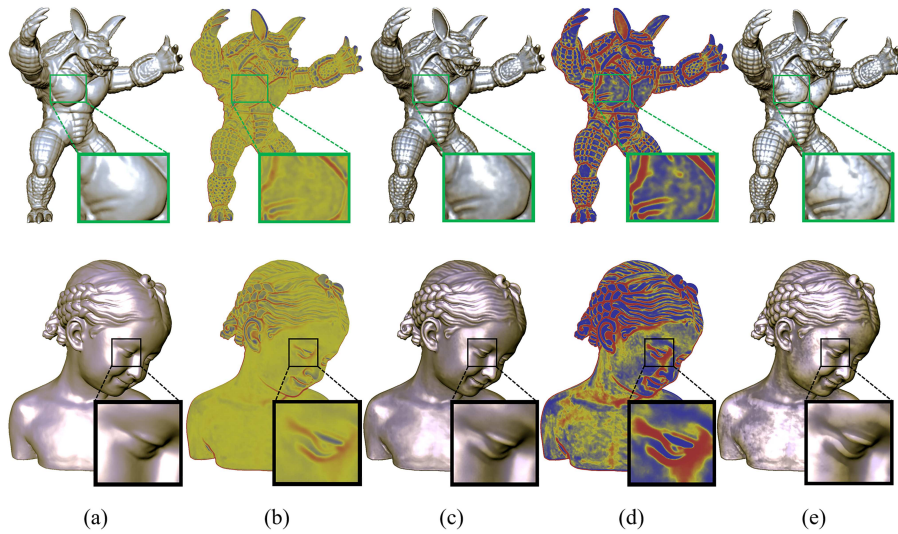


Fig. 14: Geometry-based shading technique enhances the shape depiction at multiple scales. (a) Original rendering. (b) Surface curvature are computed using 3×3 filter kernel size and then surface shape is enhanced as in (c). (d) Surface curvature are computed using 5×5 filter kernel size and then surface shape is enhanced as in (e).

Extracting surface features at multiple scales is an interesting advantage of the geometry-based shading technique. From practical point of view, it is easily adapted to the creation of levels-of-details by computing the surface curvature over extended neighbors in image space. An example of computing the surface curvature at two different scales is illustrated in Fig 14. Computing the surface curvature at small scale contributes to compellingly extracting the salient surface features where the surface details are precisely conveyed (See Fig 14-b). This can lead to properly enhancing the shape of eyes, mouth, arm, and leg of the armadillo model, as shown in Fig 14-c. Observe how our technique also provides a smooth transition between regions of wide variety of curvature information as in the close-up view of Fig 14-c.

In contrast, computing the surface curvature at large scale contributes to better separate convexities and concavities features, as well as more accurately in terms of conveying the fine surface details, as shown in Fig 14-d. As a result, Fig 14-e illustrates how the shape of eyes, mouth, arm, and leg of the armadillo model is more apparent because concavities and convexities give rise to contrasted colors which make them easily to distinguish from each other. Also, observe how various surface features of the bimba 3d model are properly enhanced in Fig 14-e: rough details around shoulders, sharp features on the hair and face. However, using large kernel size may merge some surface features due to relying on conveying the far features, as shown in the

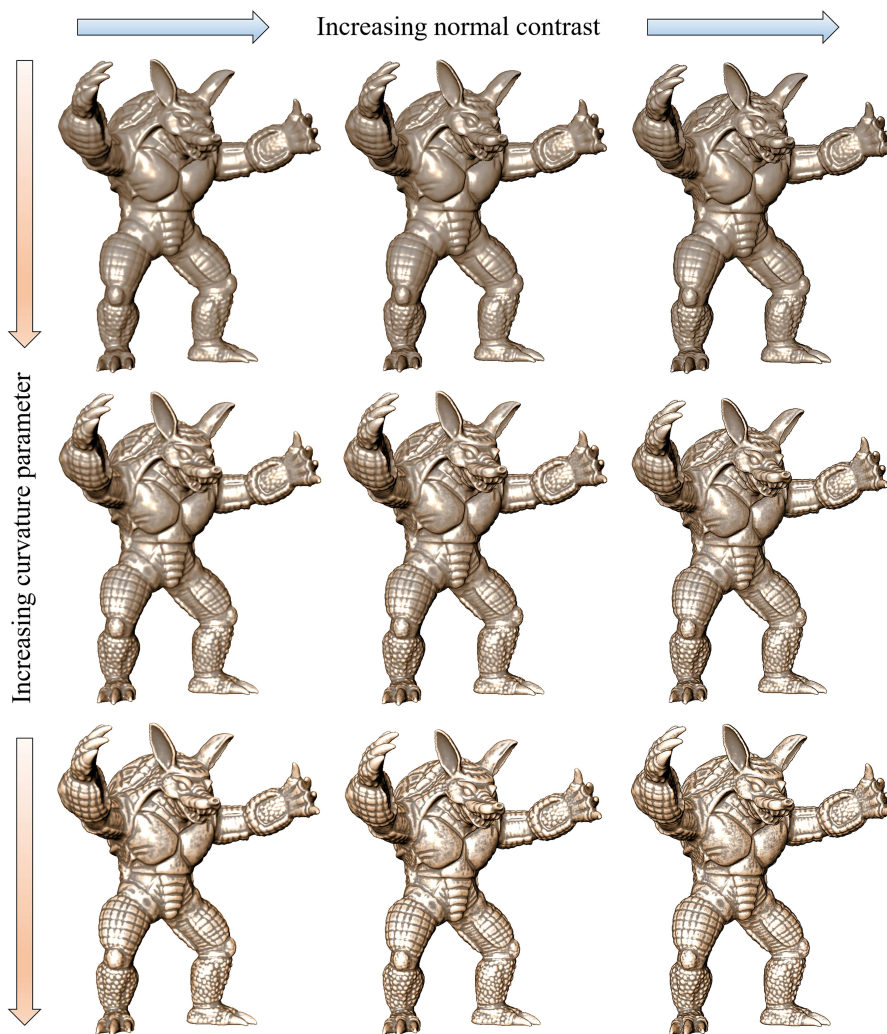


Fig. 15: Geometry-based shading technique enhances surface details in two ways to produce a more compelling result where all fine surface details are enhanced and convexities and concavities are easily distinguished from each other.

close-up views of Fig 14-d and Fig 14-e of the bimba 3d model where the planer regions are merged with concave one to produce more deeply concave regions. In a nutshell, computing the surface curvature at larger scale leads to better conveying of fine surface details, however, it may merge some surface features as well as reduce the rendering times.

In response to our motivation from combining the advantages of Normal enhancement [2] and Radiance scaling [34], we show in Fig 15, that

dual enhancement which proposed by Geometry-based shading technique is most effective in conveying the illumination characteristics, material, and surface features. More precisely, Geometry-based shading technique is efficient at modifying the surface normal to enhance the surface shading. However, this type of shading enhancement relies on a simple high-frequency enhancement operation, and as a result is not be able to enhance material characteristics and all surface details. On the other hand, Geometry-based shading technique also correlates reflected lighting intensity to surface curvature in a way that allows user to enhance concavities and convexities. Consequently, Geometry-based shading technique enhances surface shape in two different ways that complement each other in conveying geometry surface features where all fine surface details are enhanced. The dual enhancement produces a more compelling result where the local contrast of the object is enhanced and distinguishing convexities from concavities becomes easier.

8 Discussion

8.1 Performance

The performance of the Geometry-based shading technique was evaluated and compared with a radiance scaling technique [34]. The performance tests are conducted using a PC equipped with an Intel(R) Core(TM) i7-47903.6 GHz CPU, 16G host memory, and AMD FirePro W2100 graphics card. The tests are performed at same illumination settings, dataset, resolution and kernel size. Indeed, we rendered the objects using Blinn-Phong shading model under single directional light. Table 1 shows the results of our performance evaluation. The performance statistics shows that the rendering performance of Geometry-based shading technique is comparable with radiance scaling technique [34]. For small kernel size and moderate objects complexity (*Elephant and Armadillo*), both techniques perform similarly. With an increasing of object complexity and kernel size, Geometry-based shading technique is slightly inferior. This can be explained by the normal enhancement process which have been applied in prior of estimating the surface curvature. Although this process can enhance the quality of the estimated curvature, it adds a relatively small overhead and thus the real-time performance is reduced, especially with complex meshes and large kernel size. However, the performance of Geometry-based shading technique can compete with the Radiance scaling technique [33]. Observe that even the mesh size is increased 400000 Triangles, the kernel size to 77 and screen resolution to 1024768, Geometry-based shading technique still maintain a high frame rate making it suitable for interactive applications.

As explained in Table 1, the performance of Geometry-based shading technique mainly depends on three factors: The input 3D model complexity, screen resolution, and the kernel size. Observe how the performance is changed when one of these factors is altered. For instance, with replacing the

Elephant model by Armadillo model, the performance drops down from 342 fps to 285 fps using the same screen resolution and the kernel size. Extracting surface features at multiple scales is an interesting advantage of our curvature measure which may affects the rendering speed. This is easily done by computing surface curvature over extended neighborhoods in image space. Accordingly, we suggest using a reasonably large kernel size to make a trade-off between the extracted surface features and the performance efficiency.

Table 1: Performance statistics

Model	Size of Model (Vertices/Triangles)	Resolution	Kernel size	Radiance scaling (FPS)	Geometry-based shading (FPS)
Elephant	249029 / 84638	800 × 600	3	490	486
			5	426	418
			7	352	342
		1024 × 768	3	342	339
			5	296	291
			7	239	232
Armadillo	189295 / 345944	800 × 600	3	288	285
			5	265	259
			7	238	229
		1024 × 768	3	176	172
			5	208	202
			7	233	225
Bimba	203274 / 384266	800 × 600	3	271	266
			5	252	245
			7	226	218
		1024 × 768	3	220	215
			5	198	192
			7	173	165
Vase-lion	218081 / 400000	800 × 600	3	268	261
			5	251	241
			7	230	218
		1024 × 768	3	219	211
			5	186	179
			7	143	135

8.2 Qualitative comparisons with previous methods

The local shape descriptor that proposed in light warping [32] introduces enhancement abilities similar to ours in term of curvature estimation. However, their method tends to create discontinuities between convex and concave regions. The reason may be that the curvature is computed in image-space. Observe how their descriptor starts enhancing geometry tessellation, as show in Fig 16-a. Therefore, we apply a smooth blur to normal map in prior of computing the surface curvature to avoid such discontinuities, and provide a smooth transition between regions with wide variety of curvature information as shown in Fig 16-b. Compared to [32], observe how our descriptor

offers important advantages in terms of robustness to noise. Recent works [37] introduced similar ideas to our curvature estimation algorithm. However, their method is classified as object-space curvature measure, which is expensive and ignores many properties of human visual system.

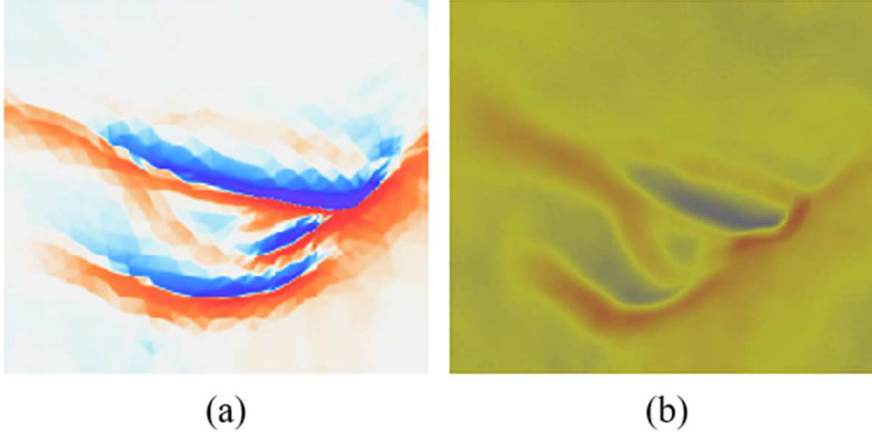


Fig. 16: Zoomed view of curvature map for bimba eye region. (a) The view-centered descriptor [32] with (red colors for concavities, blue colors for convexities and white colors for planar regions) describes the surface features with noises. (b) Our descriptor exhibits less noise while describing the surface features with red colors for concavities, blue colors for convexities and yellow for planar regions.

The Geometry-based shading technique that we introduced improves the shape depiction with arbitrary materials and styles. It may produce results similar to radiance scaling [34] or 3D gradient enhancement [37] as shown in Figs 17,18. Compared to radiance scaling [34], Geometry-based shading technique shows more convincing enhancement abilities without any constraint on the choice of material. Fig.17-a depicts how the radiance scaling enhanced the diffuse material. By observing the close-up views, we find that radiance scaling suffers in terms of transition between surface features, while geometry-based shading technique enhances the surface details with notable ability to distinguish convexities from concavities (see Fig.17-b). Although radiance scaling enhanced each lobe of the Blinn-Phong shading model independently to improve the shape depiction as shown in Fig.17-c, it suffers from allowing the user to produce results in different enhancement extent. In contrast, geometry-based shading technique offers a greater control as mapping the curvature using a non-linear function and scaling the reflectance intensity through a uniformly coherent way, which produces enhanced shading result for any choice of curvature mapping function. It also enhances the

surface shape in different ways, enabling a much wider range of enhancement abilities. Observe how various surface features of the bimba 3d model are properly enhanced in Fig.17-d: sharp features on the hair, ear and face.

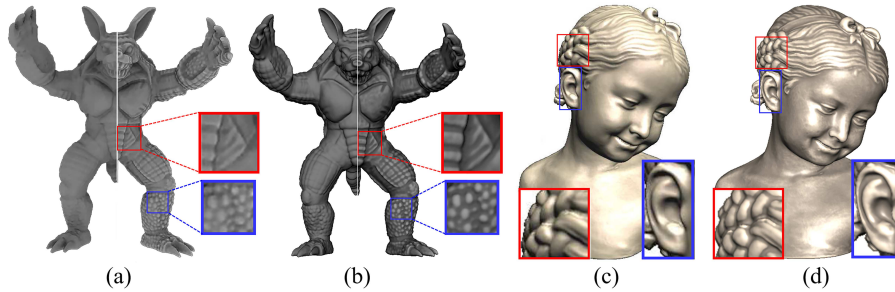


Fig. 17: Comparison with the radiance scaling technique [34]. (a) Diffuse material enhanced using radiance scaling technique [34]. (b) Diffuse material enhanced using geometry-based shading technique. (c) Each lobe of Blinn-Phongs shading model is enhanced using radiance scaling technique [34]. (d) Each lobe of Blinn-Phongs shading model is enhanced using geometry-based shading technique.

Compared to 3D gradient enhancement [37], geometry-based shading technique enhances surface features in a way that combines the advantages of curvature shading and normal enhancement. Furthermore, 3D gradient enhancement tends to flatten the overall shape perception as a result of its ability to handle the grazing angle area. Observe how Geometry-based shading technique in Fig 18-a can convey most of the salient features of the model and then correlate the reflected lighting to these features effectively. This is while 3D gradient enhancement is limited to correlating the specular material to surface features variations, which are illustrated in the red and green squares of Fig 18-b.

Toon shading style often tends to mask subtle shading variations due to the quantization of the reflected lighting intensity. This limitation clearly appears in Fig 19-a which shows the depiction of the hand 3D model using toon shading style based on [16] technique. Observe how their technique is unable to depict the wrinkles that often appear on the hand. This is in contrast to our technique, which handles this issue by depicting the concave and convex features with dark and bright colors respectively, and hence, the effectiveness of our technique still properly enhances many surface details even when using toon shading style, as shown in Fig 19-b.

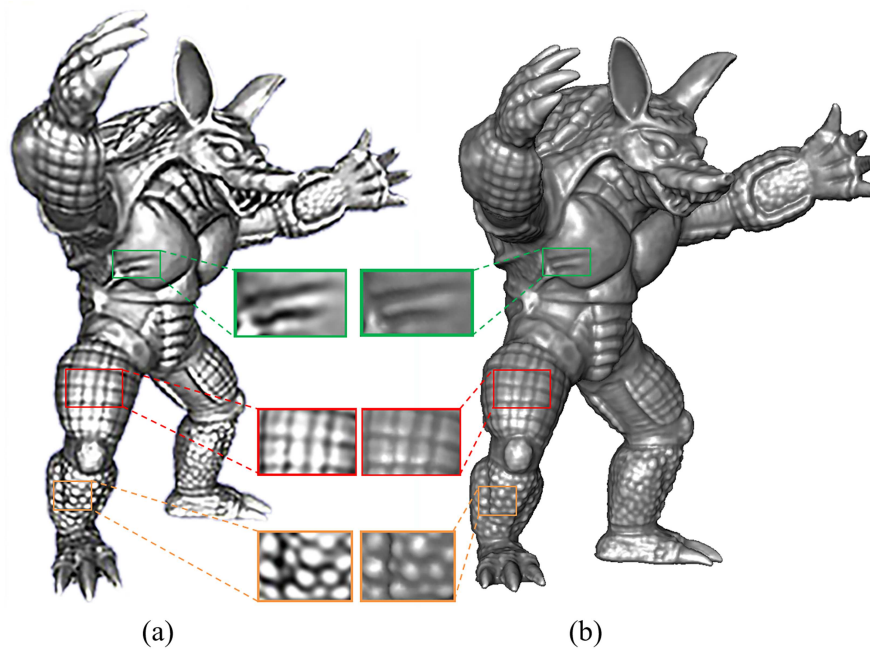


Fig. 18: Comparison with the 3D gradient enhancement [37]. (a) Armadillo model rendered with 3D gradient enhancement [37]. (b) Armadillo model rendered with geometry-based shading technique.

8.3 User study

To perform a qualitative evaluation with state-of-the-art shape depiction enhancement techniques, we carried out a user study consisting of 30 participants. The participants fall into two main categories. Professional illustrators and end users. The former represents those individuals who work on creating a good art works (with at least two years experience), and the latter represents people without drawing experiences (Computer science students). Every participant completed a questionnaire listing his/her gender, age, and number of years of art training. In all, there were 19 females and 11 males. The ages ranged from 19 to 37 years, with an average of 24. The participants were classified to 8 professional illustrators and 22 end users.

The main goal of the user study is to obtain a subjective evaluation of the images generated with the Geometry-based shading technique, in comparison to the ones obtained with original shading, Radiance Scaling [34] and 3D Gradient Enhancement [37]. Each of these techniques are represented by images have been extracted from their corresponding original papers and supplemental materials. We asked the participants to choose the best image in

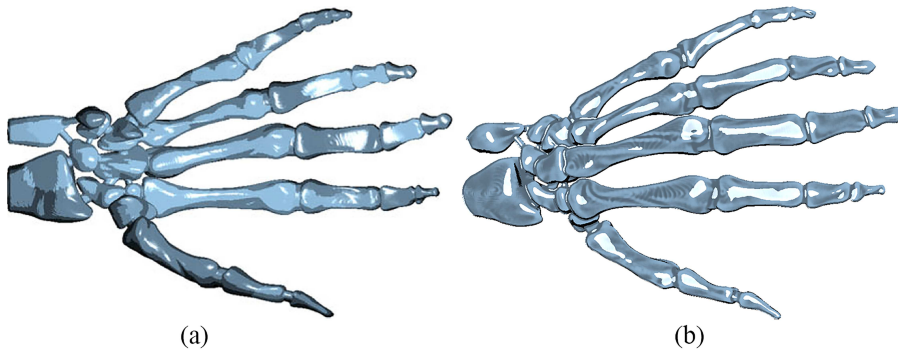
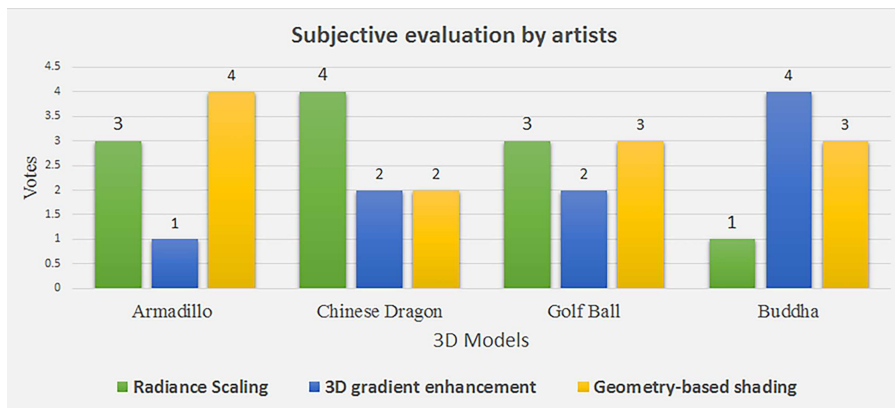


Fig. 19: Comparison with the technique proposed by Lee et al. [16]. (a) Toon shading style enhanced using [16]. (b) Toon shading style enhanced using Geometry-based shading technique.

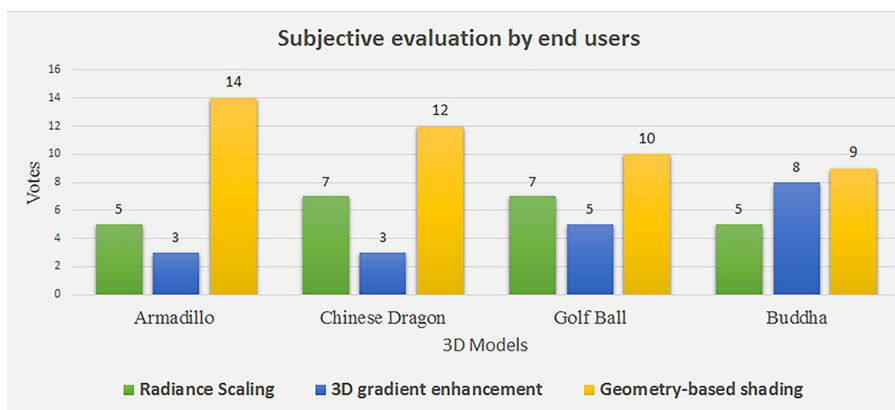
terms of aesthetic depiction. Thus, each participant should take into account two important consideration through the evaluation process.

- Illustrating the original shape correctly.
- Depicting the surface well in an aesthetic way.

In order to analyze the results and obtain the final ranking, the Schulze method is used [26]. As the aesthetic depiction is our consideration, we analyzed the results for each category of the participants. Fig.20-a shows the statistics of the user study for artists category, while Fig.20-b shows the statistics of the user study for end users category. The results show that the professional artists preferred the enhanced image produced by Geometry-based shading technique for Armadillo model, while they prefer the image that generated from radiance scaling in terms of Chinese dragon model. In context of Golf Ball model, the proposed Geometry-based shading technique and Radiance Scaling technique are obtained the same percentage of artists satisfaction, while 3D gradient enhancement technique is outperformed other techniques in terms of Buddha model. On the other hand, the results show that end users preferred Geometry-based shading technique in terms of conveying each model. Afterwards, the results for all participants are analyzed to obtain the best technique. Fig.21-a shows the statistics of the user study for all participants for each model, while Fig.21-b shows the final statistics for each technique. It is noticeable that Geometry-based shading technique is preferable by most of the participants (47.5%), followed by radiance scaling (29.2%) and finally 3D gradient enhancement (23.3%).

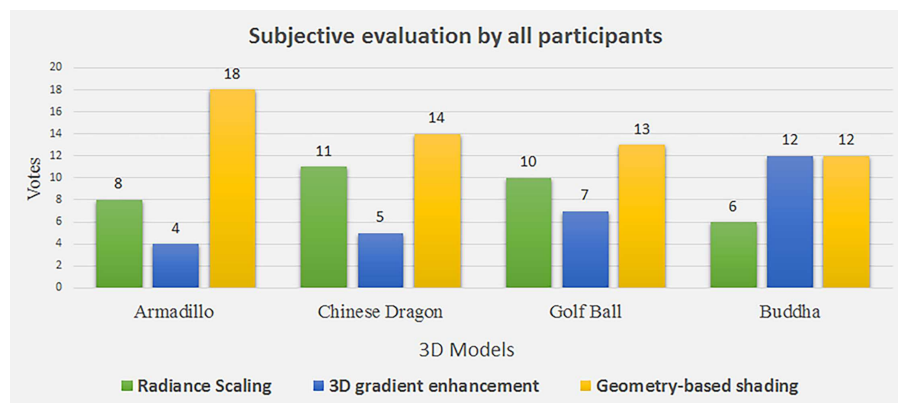


(a)

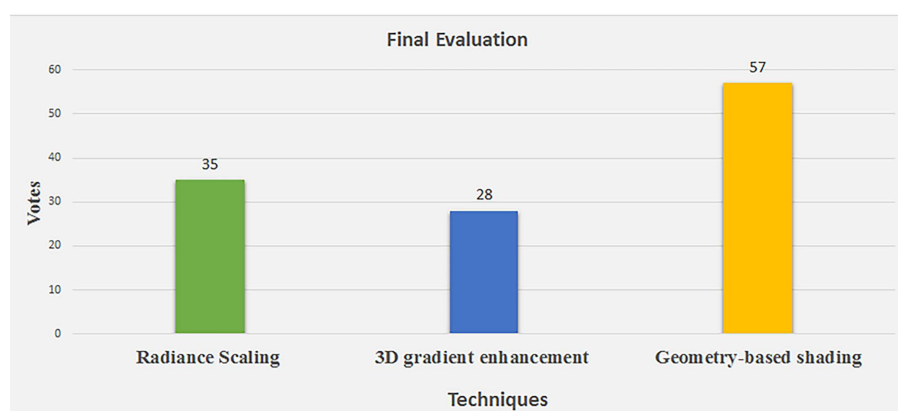


(b)

Fig. 20: The statistics of the user study for (a) Artists only. (b) End users only.



(a)



(b)

Fig. 21: (a) The statistics of the user study for all participants. (b) The final ranking of the shape depiction enhancement techniques based on the statistics of user study .

8.4 Limitations and Directions for Future Work

The Geometry-based Shading technique has some limitations though. First, although the proposed descriptor is very flexible through computing surface curvature from smoothed or exaggerated normal, our enhancement technique produces some noises as shown in Fig.22-c. This is mainly due to push the magnitude of normal sharpening parameter to exaggerated values. We suggest using a reasonably values of normal parameter to make a tradeoff between the robustness and the contrast enhancement as shown in Fig.22-a

and Fig.22-b. This is mainly due to amplifying the high-frequency components of the surface normal. Second, although the proposed curvature mapping function has two parameters to control the curvature mapping over 3D surface model, there is still room for making some improvements. Indeed, the proposed Curvature-based Reflectance Scaling Function tends to exaggerate shading transitions when curvature magnitude parameter is pushed to exaggerated values. Finally, normal enhancement process adds a relatively small overhead which reduces the real-time performance especially with large meshes. Concerning the real-time performance issue, we plan to propose a fast normal enhancement method in the future. Indeed, when the fast normal enhancement method is incorporated into Geometry-based Shading technique, a new solution for increasing performance is proposed.

Other directions for future work is to apply our work to various illumination settings such as Ashikmin model under environment lighting, as we believe in the ability of our approach of producing enhanced NPR style under this type of illumination. Moreover, we would like to make use of the proposed descriptor for depicting the shape through line drawings in a way that correlating line drawings style to surface features variations.

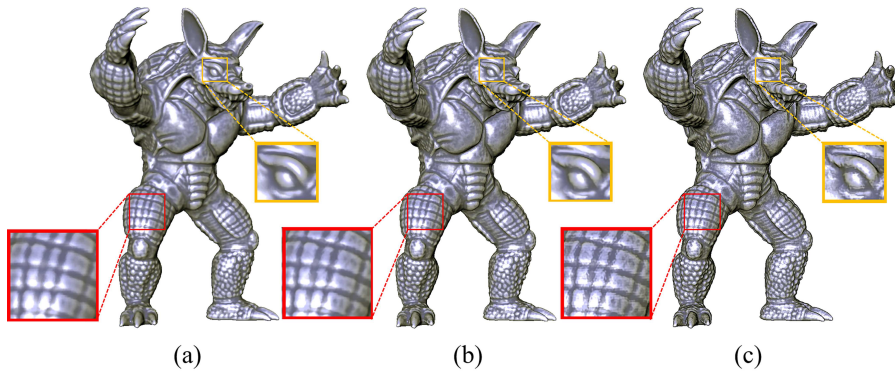


Fig. 22: Armadillo 3D model enhanced by Geometry-based Shading technique using three normal enhancement parameters. (a) Our enhanced result using normal smoothing parameter (b) Our enhanced result using reasonably values of normal sharpening parameter. (c) Our enhanced result using extreme values of normal sharpening parameter.

9 Conclusion

We have introduced a shape depiction enhancement technique called Geometry based Shading technique that convey more artistic drawings principles while preserving material and illuminating characteristics. Compared to previous approaches, more shape depiction functionalities are gained such as

controlling levels-of-details, robustness to noise, real-time rendering on the GPU and naturally coherent manner to enhance shape depiction with various illumination settings and material characteristics. To illustrate the proposed technique potential, we demonstrated its use with three non-photorealistic rendering styles, including intuitive and efficient ways to control the depiction of 3D objects shape.

References

1. Anjyo Ki, Wemler S, Baxter W (2006) Tweakable light and shade for cartoon animation. In: Proceedings of the 4th international symposium on Non-photorealistic animation and rendering, ACM, pp 133–139
2. Cignoni P, Scopigno R, Tarini M (2005) A simple normal enhancement technique for interactive non-photorealistic renderings. *Computers & Graphics* 29(1):125–133
3. DeCarlo D, Finkelstein A, Rusinkiewicz S, Santella A (2003) Suggestive contours for conveying shape. *ACM Transactions on Graphics (TOG)* 22(3):848–855
4. Decaudin P (1996) Cartoon-looking rendering of 3d-scenes. Syntim Project Inria 6
5. Fleming RW, Torralba A, Adelson EH (2004) Specular reflections and the perception of shape. *Journal of Vision* 4(9):10–10
6. Fleming RW, Torralba A, Adelson EH (2009) Three dimensional shape perception, chapter shape from sheen
7. Gooch A, Gooch B, Shirley P, Cohen E (1998) A non-photorealistic lighting model for automatic technical illustration. In: Proceedings of the 25th annual conference on Computer graphics and interactive techniques, ACM, pp 447–452
8. Hao W, Wang Y (2013) Saliency-guided luminance enhancement for 3d shape depiction. In: Virtual Reality and Visualization (ICVRV), 2013 International Conference on, IEEE, pp 9–14
9. Hogarth B (1991) Dynamic Light and Shade. ERIC
10. Judd T, Durand F, Adelson E (2007) Apparent ridges for line drawing. In: *ACM transactions on graphics (TOG)*, ACM, vol 26, p 19
11. Kajiya JT (1986) The rendering equation. In: *ACM Siggraph Computer Graphics*, ACM, vol 20, pp 143–150
12. Kindlmann G, Whitaker R, Tasdizen T, Moller T (2003) Curvature-based transfer functions for direct volume rendering: Methods and applications. In: Visualization, 2003. VIS 2003. IEEE, IEEE, pp 513–520
13. Kolomenkin M, Shimshoni I, Tal A (2008) Demarcating curves for shape illustration. In: *ACM Transactions on Graphics (TOG)*, ACM, vol 27, p 157
14. Lake A, Marshall C, Harris M, Blackstein M (2000) Stylized rendering techniques for scalable real-time 3d animation. In: Proceedings of the

- 1st international symposium on Non-photorealistic animation and rendering, ACM, pp 13–20
15. Lee CH, Hao X, Varshney A (2006) Geometry-dependent lighting. *IEEE Transactions on Visualization and Computer Graphics* 12(2):197–207
 16. Lee J, Kim S, Kim SJ (2015) Mesh segmentation based on curvatures using the gpu. *Multimedia Tools and Applications* 74(10):3401–3412
 17. Lee Y, Markosian L, Lee S, Hughes JF (2007) Line drawings via abstracted shading. In: *ACM Transactions on Graphics (TOG)*, ACM, vol 26, p 18
 18. Miao Y, Feng J, Pajarola R (2011) Visual saliency guided normal enhancement technique for 3d shape depiction. *Computers & Graphics* 35(3):706–712
 19. Miao YW, Feng JQ, Wang JR, Pajarola R (2012) A multi-channel salience based detail exaggeration technique for 3d relief surfaces. *Journal of Computer Science and Technology* 27(6):1100–1109
 20. Ohtake Y, Belyaev A, Seidel HP (2004) Ridge-valley lines on meshes via implicit surface fitting. *ACM transactions on graphics (TOG)* 23(3):609–612
 21. Pharr M, Green S (2004) Ambient occlusion. *GPU Gems* 1:279–292
 22. Ritschel T, Smith K, Ihrke M, Grosch T, Myszkowski K, Seidel HP (2008) 3d unsharp masking for scene coherent enhancement. In: *ACM Transactions on Graphics (TOG)*, ACM, vol 27, p 90
 23. Rusinkiewicz S (2004) Estimating curvatures and their derivatives on triangle meshes. In: *3D Data Processing, Visualization and Transmission, 2004. 3DPVT 2004. Proceedings. 2nd International Symposium on*, IEEE, pp 486–493
 24. Rusinkiewicz S, Burns M, DeCarlo D (2006) Exaggerated shading for depicting shape and detail. In: *ACM Transactions on Graphics (TOG)*, ACM, vol 25, pp 1199–1205
 25. Saito T, Takahashi T (1990) Comprehensible rendering of 3-d shapes. In: *ACM SIGGRAPH Computer Graphics*, ACM, vol 24, pp 197–206
 26. Schulze M (2011) A new monotonic, clone-independent, reversal symmetric, and condorcet-consistent single-winner election method. *Social Choice and Welfare* 36(2):267–303
 27. Todo H, Anjyo Ki, Baxter W, Igarashi T (2007) Locally controllable stylized shading. *ACM Transactions on Graphics (TOG)* 26(3):17
 28. Todo H, Anjyo K, Yokoyama S (2013) Lit-sphere extension for artistic rendering. *The Visual Computer* 29(6-8):473–480
 29. Toler-Franklin C, Finkelstein A, Rusinkiewicz S (2007) Illustration of complex real-world objects using images with normals. In: *Proceedings of the 5th international symposium on Non-photorealistic animation and rendering*, ACM, pp 111–119
 30. Vanderhaeghe D, Vergne R, Barla P, Baxter W (2011) Dynamic stylized shading primitives. In: *Proceedings of the ACM SIGGRAPH/Eurographics Symposium on Non-Photorealistic Animation and Rendering*, ACM, pp 99–104

31. Vergne R, Barla P, Granier X, Schlick C (2008) Apparent relief: a shape descriptor for stylized shading. In: Proceedings of the 6th international symposium on Non-photorealistic animation and rendering, ACM, pp 23–29
32. Vergne R, Pacanowski R, Barla P, Granier X, Schlick C (2009) Light warping for enhanced surface depiction. In: ACM Transactions on Graphics (TOG), ACM, vol 28, p 25
33. Vergne R, Pacanowski R, Barla P, Granier X, Schlick C (2010) Radiance scaling for versatile surface enhancement. In: Proceedings of the 2010 ACM SIGGRAPH symposium on Interactive 3D Graphics and Games, ACM, pp 143–150
34. Vergne R, Pacanowski R, Barla P, Granier X, Shlick C (2011) Improving shape depiction under arbitrary rendering. IEEE Transactions on visualization and computer graphics 17(8):1071–1081
35. Xie X, He Y, Tian F, Seah HS, Gu X, Qin H (2007) An effective illustrative visualization framework based on photic extremum lines (pels). IEEE Transactions on Visualization and Computer Graphics 13(6):1328–1335
36. Zhang L, He Y, Xia J, Xie X, Chen W (2011) Real-time shape illustration using laplacian lines. IEEE Transactions on visualization and Computer Graphics 17(7):993–1006
37. Zhao F, Liu X (2014) 3d gradient enhancement. The Visual Computer 30(1):113–126
38. Zhao H, Jin X, Mao X (2013) Real-time directional stylization of images and videos. Multimedia tools and applications 63(3):647–661